HEFAT2010
7th International Conference on Heat Transfer, Fluid Mechanics and Thermodynamics
19-21 July 2010
Antalya, Turkey

LATTICE BOLTZMANN ANALYSIS OF LAMINAR FORCED CONVECTION IN A PLANE CHANNEL WITH A BUILT-IN TRIANGULAR PRISM

[1]Benim A.C*, [2]Aslan, E., and [2]Taymaz, I.
*Author for correspondence
[1]Department of Mechanical and Process Engineering,
Duesseldorf University of Applied Sciences,
Josef-Gockeln-Str. 9, D-40474 Duesseldorf,
Germany,
[2]Department of Mechanical Engineering,
Sakarya University, Sakarya,
Turkey.

ABSTRACT

The Lattice Boltzmann Method (LBM) is employed to computationally analyze the incompressible, laminar flow and heat transfer for a fluid with constant material properties, in a two-dimensional channel with a built-in triangular prism. In addition to the momentum transfer, the energy transfer is also modeled by LBM. A uniform lattice structure, along with a single time relaxation approach is employed. Predictions are obtained for different Reynolds numbers while keeping the Prandtl number at the value of 0.71. For validating the developed LBM code, the predictions are compared with those obtained by a commercial CFD code. It is observed that the present LBM code delivers results that are of comparable accuracy to the well-established CFD code. Results show that the presence of a triangular prism affects the flow and heat transfer patterns for the steady-state (for the lower Reynolds numbers) and unsteady-periodic (for the investigated Reynolds number values larger than 500) flow regimes. It is observed that heat transfer to channel walls can be enhanced by the triangular prism, especially for the higher Reynolds numbers, exhibiting an unsteady-periodic flow structure. The latter is identified to be the main mechanism responsible for heat transfer enhancement. It is also demonstrated that the error in the predictions can be quite large, if this flow unsteadiness is artificially suppressed by employing a symmetry plane through mid-channel (although the time-averaged flow field is symmetric).

INTRODUCTION

Flow and heat transfer in pipes and channels with built-in bluff bodies have been investigated by many researchers, both experimentally [1] and computationally [2]. Because this flow configuration is important and encountered in different applications concerning heat exchange systems.

Within this coverage, a triangular prism can be considered to be a basic bluff body configuration. Abbasi et al. [3] computationally investigated the incompressible laminar flow and heat transfer in a planar channel with a built-in triangular prism. They demonstrated that the employment of a triangular prism could improve the heat transfer to the channel walls. Chattopadhyay [4] numerically analyzed a similar configuration, for the incompressible turbulent flow, by applying a steady-state (Reynolds Averaged Navier-Stokes Equations, RANS) analysis based on a two-equation turbulence model. The previous numerical analysis [2-4] was exclusively based on the discretization of the Navier-Stokes equations. The originality of the present contribution is the application of the Lattice Boltzmann Method (LBM) [5] to investigate the problem. The presently developed two-dimensional LBM code for incompressible flows, which was recently applied [6] to several benchmark isothermal, steady-state flow problems. This code is now extended to include the transport of thermal energy, and applied to solve the present problem. The present results are compared with those obtained by the commercial CFD code Fluent [7].

Quite recently [8], a similar problem, namely, the forced convection in a plane-channel with built-in square obstacles was analyzed by LBM. However, in that investigation [8], the flow field was modeled by LBM, whereas the continuum's energy equation was discretized by the finite difference method. In contrast to the previous work [8], the temperature distribution is also computed by LBM, in the present analysis.

NOMENCLATURE

a	[m^2/s]	Thermal diffusivity
B	[m]	Base of triangular prism cross section
c	[m/s]	Speed

c_p	[J/kgK]	Isobaric specific heat capacity
c_s	[m/s]	Lattice sound speed
D_h	[m]	Hydraulic diameter
$\vec{e}_\alpha$	[m/s]	Discrete velocity set
f_α	[kg/m^3]	Discrete density distribution function
g_α	[K]	Discrete temperature distribution function
H	[m]	Channel height
h	[W/m^{2}K]	Heat transfer coefficient ($h=q/(T_W-T_{F,0})$)
k	[W/mK]	Thermal conductivity
Nu	[-]	Nusselt number ($Nu=hD_h/k$)
p	[Pa]	Static pressure
p_0	[Pa]	Reference static pressure
Pr	[-]	Prandtl number ($Pr=\mu c_p/k$)
q	[W/m^2]	Heat flux
Re	[-]	Reynolds number ($Re=\rho u_0 D_h/\mu$)
T	[K]	Temperature
t	[s]	Time
u	[m/s]	Axial velocity
u_0	[m/s]	Mean inlet velocity
$\vec{x}$	[m]	Position vector
x, y	[m]	2D Cartesian coordinates

Greek symbols

δ	[m]	Lattice unit (distance between neighbouring nodes)
δt	[s]	Time step
μ	[Pa.s]	Dynamic viscosity
ν	[m^2/s]	Kinematic viscosity
ρ	[kg/m^3]	Density
ρ_0	[kg/m^3]	Reference density
ω	[-]	Collision frequency for momentum transfer
ω_T	[-]	Collision frequency for energy transfer

Sub- and superscripts

F	Fluid
eq	Equilibrium value
W	Wall
0	Inlet
$\sim$	Post collision state

DEFINITION OF THE PROBLEM

The present geometry is similar to the one used by Abbasi et al. [3] in their analysis based on a Control Volume based Finite Element Method. A sketch of the geometry is shown in Figure 1.

The geometry and boundary conditions are symmetric around a plane at the channel mid-height, running through the middle of the triangular prism. Thus, a modelling approach could be to utilize this symmetry, and solve the equations only for the half of the channel Nevertheless, although the time-averaged flow is symmetric, the time-dependent flow may not be. Indeed, the latter is instantaneously asymmetric due to periodic vortex shedding behind the prism, for most Reynolds numbers, except a small range of low values. Thus, an a-priori use of a symmetry plane, which artificially suppresses the unsteady motion, independently from the Reynolds number, can lead to errors, as the results of such an enforced symmetric, steady-state solution can differ from the symmetric, time-averaged flow field of an unsteady computation.

Nevertheless, a symmetry plane can be used, for sufficiently low Reynolds numbers that "physically" have a steady-state solution. Such a symmetry plane can intentionally be used also for high Reynolds numbers, for purposes numerical investigations (without claiming physical accuracy), as also practiced within the present study.

For the momentum equations, a fully developed, parabolic

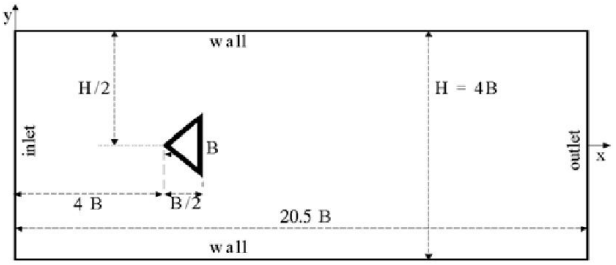

Figure 1 Solution domain, boundary types.

channel flow velocity profile is imposed as boundary condition at the inlet. At the outlet, a constant static pressure is prescribed. No-slip boundary conditions hold at the solid walls. For the energy equation temperature is prescribed to be constant at the inlet boundary. Walls of the triangular prism are assumed to be adiabatic. At the outlet, zero-gradient boundary conditions are applied.

MATHEMATICAL AND NUMERICAL FORMULATION

As it is the case for the most LBM applications, the Bhatangar-Gross-Krook (BGK) [9] single relaxation time approximation is adopted. In the present investigation, such a version [10] of the approach is applied, which is especially suitable for unsteady, incompressible flows. For the momentum and energy transport, both, the 2-dimensional 9-velocity lattice model (D2Q9) is used, which is sketched in Figure 2.

In agreement with the original idea underlying LBM, a uniform lattice structure is used. This gives rise to an orthogonal and in both directions equidistant (square shaped) lattice pattern. In the open literature, various applications of LBM can be found, where non-equidistant, or even unstructured computational grids are used in conjunction with LBM, where LBM is amended with various interpolation techniques [11,12].

Similarly, there are multiple time relaxation (MTR) approaches, which allow greater values of the collision frequency to be used [13], as the maximum allowed values of the collision frequency are limited by stability limits. Nevertheless, in the present investigation, it is preferred to work with the "classical" LBM formulation using the square shaped lattice structures directly as the computational grid, without recourse to interpolation procedures to, as well as a single time relaxation scheme, leaving the topics of non-equidistant / unstructured grids and multiple time relaxation for the future work.

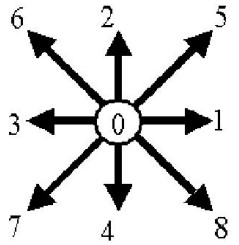

Figure 2 D2Q9 lattice model

Two different distribution functions, one for density (momentum) and the other for the temperature are used. The discretized lattice Boltzmann evolution equations for momentum and energy transport, which are usually solved in two consecutive steps, i.e. in a "collision" and a following "streaming" step, are provided below:

Collision:

$$\tilde{f}_\alpha(\vec{x},t+\delta t) = f_\alpha(\vec{x},t) - \omega\left[f_\alpha(\vec{x},t) - f_\alpha^{eq}(\vec{x},t)\right] \quad (1a)$$

$$\tilde{g}_\alpha(\vec{x},t+\delta t) = g_\alpha(\vec{x},t) - \omega_T\left[g_\alpha(\vec{x},t) - g_\alpha^{eq}(\vec{x},t)\right] \quad (1b)$$

Streaming:

$$f_\alpha(\vec{x}+\vec{e}_\alpha\delta t, t+\delta t) = \tilde{f}_\alpha(\vec{x},t+\delta t) \quad (2a)$$

$$g_\alpha(\vec{x}+\vec{e}_\alpha\delta t, t+\delta t) = \tilde{g}_\alpha(\vec{x},t+\delta t) \quad (2b)$$

The collision frequencies are defined by

$$\omega = \frac{1}{\frac{\nu}{c_s^2\,\delta t}+\frac{1}{2}} \quad (3a)$$

$$\omega_T = \frac{1}{\frac{a}{c_s^2\,\delta t}+\frac{1}{2}} \quad (3b)$$

where the lattice sound speed c_s is defined as

$$c_s = \frac{c}{\sqrt{3}} \quad (4)$$

with the lattice speed c:

$$c = \frac{\delta}{\delta t} \quad (5)$$

The nine discrete velocities of the model are given by

$$\vec{e}_\alpha = c\begin{bmatrix} 0 & 1 & 0 & -1 & 0 & 1 & -1 & -1 & 1 \\ 0 & 0 & 1 & 0 & -1 & 1 & 1 & -1 & -1 \end{bmatrix} \quad (6)$$

The equilibrium distribution functions are given as

$$f_\alpha^{eq} = w_\alpha\left\{\rho + \rho_0\left[\frac{3}{c^2}\vec{e}_\alpha\cdot\vec{u} + \frac{9}{2c^4}(\vec{e}_\alpha\cdot\vec{u})^2 - \frac{3}{2c^2}\vec{u}\cdot\vec{u}\right]\right\} \quad (7a)$$

$$g_\alpha^{eq} = w_\alpha T\left[1+\frac{3}{c^2}\vec{e}_\alpha\cdot\vec{u}\right] \quad (7b)$$

with

$$w_\alpha = \begin{bmatrix} \frac{4}{9} & \frac{1}{9} & \frac{1}{9} & \frac{1}{9} & \frac{1}{9} & \frac{1}{36} & \frac{1}{36} & \frac{1}{36} & \frac{1}{36} \end{bmatrix} \quad (8)$$

The macroscopic fields are obtained from

$$p_\alpha = c_s^2 f_\alpha \quad (9a)$$

$$p_\alpha^{eq} = c_s^2 f_\alpha^{eq} \quad (9b)$$

$$p = \sum_{\alpha=0}^{8} p_\alpha = \sum_{\alpha=0}^{8} p_\alpha^{eq} \quad (9c)$$

$$\vec{u} = \frac{1}{p_0}\sum_{\alpha=0}^{8}\vec{e}_\alpha p_\alpha = \frac{1}{p_0}\sum_{\alpha=0}^{8}\vec{e}_\alpha p_\alpha^{eq} \quad (10)$$

$$T = \sum_{\alpha=0}^{8} g_\alpha = \sum_{\alpha=0}^{8} g_\alpha^{eq} \quad (11)$$

The time step size δt is chosen in such a manner that it results in a lattice speed c (5) of unity, which, in turn, results in a lattice sound speed in magnitude of $c_s = 1/\sqrt{3}$ (4).

The implementation of the boundary conditions are not discussed here in detail, for the sake of brevity, but can be found elsewhere [5,14]. For modelling the boundaries, the so-called "on-grid" formulation is used, where the boundary lattice grid lines are defined to be aligned with the "real" boundaries of the solution domain. At solid walls, the so-called "bounce-back" boundary condition is applied for the momentum equations. The boundary conditions are applied by accordingly prescribing the corresponding boundary values of the distribution functions [5,14]. For coding the model, sample Fortran codes provided in [14] are used as a basis.

Due to the presently applied LBM formulation, the resulting lattice structures are always square shaped, for all of the considered cases. In some cases, comparisons with the commercial CFD code Fluent [7] are presented. For a better comparability of the accuracy, the finite volume grids for the Fluent computations are also generated as principally square shaped grids, in an analogous manner to the used lattice structure. The only "local" exception is the representation of the shape of the triangular cross-section: In LBM, the triangular shape is approximated by a staircase lattice structure, whereas it is accurately resolved by the finite volume grid for the Fluent computations by using a locally unstructured configuration, but still, keeping a comparable resolution to the LBM lattice used.

In LBM, no special procedure is applied for the treatment of convection. In the Fluent computations, a possibly high accurate procedure, i.e. a Second Order Upwind procedure is used [7] in discretizing the convective terms. Furthermore, for handling the pressure-velocity coupling, the SIMPLEC method is used for the stationary computations, whereas the PISO algorithm is used for the unsteady calculations by Fluent [7]. In all Fluent calculations, basically, the default under-relaxation factors are used, that are 1.0 for the pressure, 0.7 for the

velocity components and, chosen to be 1.0 for the temperature. As convergence criteria, hundred times smaller tolerances for the scaled residuals are required than the default settings (for the energy equation smaller than 10^{-8}, for all remaining equations smaller than 10^{-5}) in Fluent calculations.

LBM is an intrinsically unsteady method, where, a stationary solution, if it exists, is found as the result of an integration in time. The procedure described by Eqs. (1,2) may be considered, in a sense, to be similar to an explicit time integration in terms of a finite volume formulation. In the unsteady analysis performed by Fluent, a Second Order Implicit time [7] integration scheme is applied. Always the same time step size is used for LBM and Fluent computations. In the unsteady calculations, the flow from any initial distribution is calculated for a period of time, which is long enough to get a periodic flow structure to be established. Subsequently, the results are time averaged, for a sufficiently long time for getting time-independent time-averaged values.

RESULTS

Preliminary Validation

The present LBM code was validated for steady-state, incompressible, laminar flows [6]. The current study represents an improvement of the code in two aspects: (1) heat transfer is included, (2) unsteady flows are analyzed, along with the implementation of an "incompressible" formulation convenient for unsteady flows [10]. Before starting with the analysis of the main problem (channel with triangular prism) an analysis is performed for a simple (classical) channel flow, without any obstacles, for an initial validation of the implementation of the heat transfer: Laminar forced convection is investigated for a fully developed channel flow. A simple channel geometry (without a triangular prism) is modelled (using 25 lattice units along half channel height) for Re = 160, with a constant inlet and a constant wall temperature. The inlet velocity profile is prescribed to be of a fully-developed channel flow. The channel length is defined to be long enough to allow a thermally fully developed flow to be established [15].

Table I compares the predicted and theoretical Nusselt numbers (Nu). Please note that the Nu used here is based on an h definition that differs form the one given in Nomenclature. Here, the fluid temperature (used to compute the temperature difference for calculating h) is taken to be the local bulk value at the corresponding cross-section in accordance with the related theory [15] (whereas this is taken to be the inlet fluid temperature in following sections, as given in Nomenclature). In Table I, one can see that a very good agreement between the LBM prediction and the theoretical value is observed, which implies the adequateness of the implementation.

On the Staircase Approximation of the Triangular Shape

With the squarish lattice structure, the shape of the rectangular prism can only be approximated by a staircase. In this section, the influence of this approximation on the accuracy is investigated. The analysis is performed for the stationary flow, assuming a symmetry boundary through the middle of the prism (Fig. 1) (since the computation does not aim at a physically accurate solution, but tries to quantify the influence

Table I Nu in fully developed channel flow (without prism)

	LBM prediction	Theory [15]
Nu	7.55	7.54

of an approximation on the numerical results, by comparing them, an artificial suppression of an eventual flow unsteadiness by a symmetry plane, is justified, within this context).

The problem is solved for Re = 100. For this comparison, only the momentum equations are solved, without considering heat transfer. Denoting the number of lattice units / finite volumes along height of the triangular cross section by N, four different grid resolutions, namely grids with N=4, 8, 12 and 16 are analyzed. Figure 3 shows the detail grids in the near-field of the triangular prism for N=8, for LBM and Fluent calculations.

Predicted variations of axial velocity along the axial distance at channel-mid height are shown in Figure 4. In the figure, one can see that the Fluent N=4 predictions exhibit a deviation from the remaning curves. For N=16, LBM and Fluent curves agree very well, indicating an accurate enough resolution of the geometry by LBM. As N=8,12 results (not shown) also agree very well with N=16, a grid independency at N=16 can also be assumed. Such comparisons are done for different Re, and also by monitoring different variables. The finally applied resolution for the main computations corresponds to N=25.

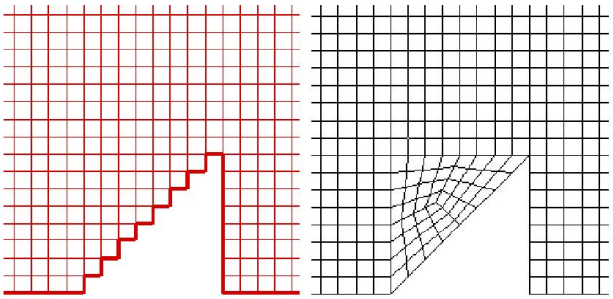

Figure 3 Grids for N=8, for Re=100: Left: LBM, Right: Fluent

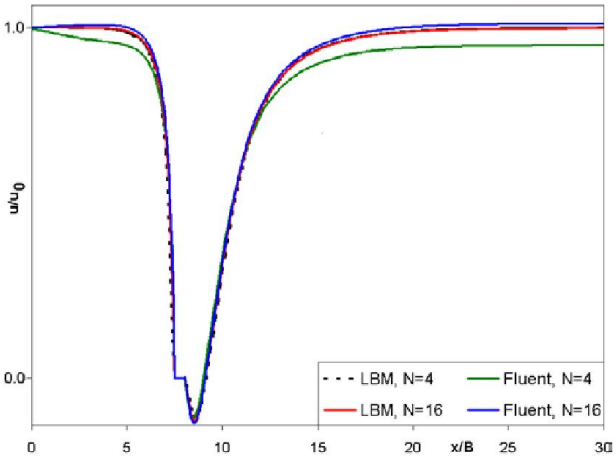

Figure 4 Variation of u with x along channel mid-height (symmetry plane, steady flow) for Re = 100.

Main Computations

Calculations are performed for Re=160,270,530,800 and 1070. It is observed that the flow converges to a steady-state solution for Re=160 and 270 (using the full channel domain, without introducing a symmetry plane). An unsteady behaviour is observed for the higher Reynolds numbers, i.e. for Re=530, 800,1070. However, also for those Reynolds numbers, stationary solutions are artificially obtained by employing the symmetry plane, for better demonstrating the error done by neglecting flow unsteadiness, and the effect of unsteady motion on the wall heat transfer. In all unsteady computations (LBM and Fluent), the time-step size applied can be considered to be fairly small (e. g. a period of the prism lift force oscillation was resolved by at least 1000 time steps). Maximum cell Courant numbers [16] were about 0.2. With the applied grid resolution (N=25), the resulting maximum cell Peclet numbers were about 10, for the highest Reynolds number, i.e. for Re=1070, which indicates that some influence of numerical diffusion can be expected in the Fluent results, depending on the Reynolds number, although a second order upwind scheme is used.

Velocity fields

Figure 5 illustrates, in the near-field of the triangular prism, the unsteady-instantaneous streamlines, the unsteady-time-averaged streamlines, and the steady-state streamlines, as predicted by LBM for Re = 800 (the steady state streamlines are obtained by applying a symmetry plane through the middle of the channel, as discussed above). The instantaneous streamlines demonstrate the unsteady flow behind the prism, due to the periodic vortex-shedding, which is not symmetric (around the channel mid-plane) at any time (Fig. 5 (a)). The streamlines of the time-averaged velocity field is seen to be symmetric around the channel mid-plane, of course, and shows a rather small recirculation zone behind the prism (Fig. 5 (b)). If the flow unsteadiness is ignored, and a stationary flow is enforced by suppressing the unsteady-periodic motion artificially, by a symmetry plane, the size of the recirculation zone is highly over-predicted (Fig. 5 (c)).

Temperature fields

LBM predicted isotherms for Re=800 are illustrated in Figure 6. The unsteady-periodic structure of the temperature field can be observed in Fig. 6a. One can also see that the temperature field of the (artificial) steady-state solution (Fig. 6c) does not differ much from that of the case without prism (Fig. 6d) except in prism's near-field, and does either not necessarily imply a substantial heat transfer enhancement. Time-averaged results of the unsteady solution (Fig. 6b) differ from the latter and indicate a more remarkable heat transfer enhancement compared to the case without prism (Fig. 6d).

Heat Transfer

Predicted variations of the Nusselt number along the channel wall, for Re=160, are presented in Figure 7. One can see that the existence of the triangular prism causes an increase in Nu in regions near the prism (3<x/B<9). This is due to the increased near-wall velocities because of the blockage. The transient phenomena does not play a role here, as a steady-flow is predicted for this Re. It is interesting to note that the Nu values with prism fall slightly below those of without prism beyond x/B>9 (caused by a flow deceleration following the acceleration in the prism region). Still, an increase of the mean

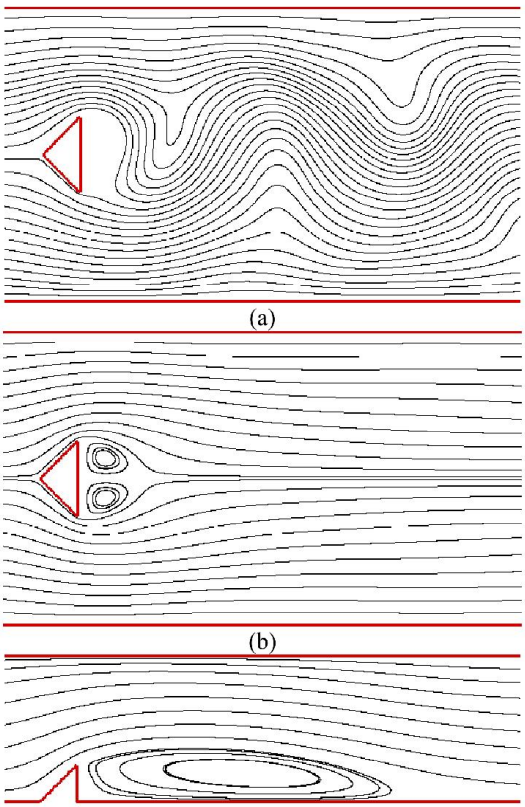

Figure 5 Predicted (LBM) streamlines for Re = 800 (a) unsteady-instantaneous, (b) unsteady-time-averaged, (c) steady-state using symmetry plane.

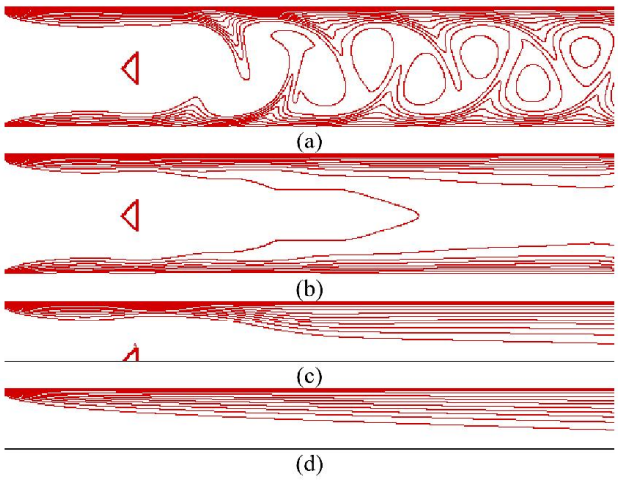

Figure 6 Predicted (LBM) isotherms for Re = 800 (a) unsteady -instantaneous, (b) unsteady-time-averaged, (c) steady-state using symmetry plane, (d) channel without prism (steady-state).

Nu by the prism is observed. One can also see that the LBM predictions agree perfectly well with the Fluent predictions.

Nu variations along the channel wall predicted for Re=800 are illustrated in Figure 8. Here, the flow is unsteady/periodic. Results neglecting the unsteadiness of the flow, i.e. steady-state results obtained by an artificial symmetry plane, show an increase of Nu in the area of the triangular prism, purely due to the increased skin friction by the blockage. Here, the local undershoot of Nu values below those of the case without prism is more strongly predicted. Nevertheless, a higher mean Nu value is still predicted. However, since the flow is unsteady, the artificially obtained stationary results do not have much physical significance (and can be quite incorrect, as seen in the comparison). The variation of the instantaneous Nu and the time-averaged Nu are also displayed in the figure. The time-averaged Nu variation shows a local peak nearly at the same location as the stationary solution, which is but, slightly lower. This is followed by a secondary local peak slightly downstram. It is interesting to see that the time-averaged Nu values are much higher than those of the case without prism and those of the stationary computation, especially in the downstream region of the prism. Thus, one can see that the heat transfer to channel walls can be enhanced by a triangular prism, and this effect is mainly due to the unsteady-periodic vortex shedding. Again, a perfect agreement with the Fluent predictions is observed.

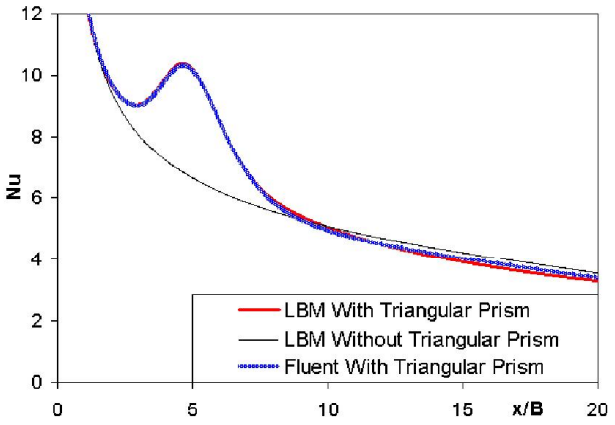

Figure 7 Predicted Nu variations along channel wall, Re=160.

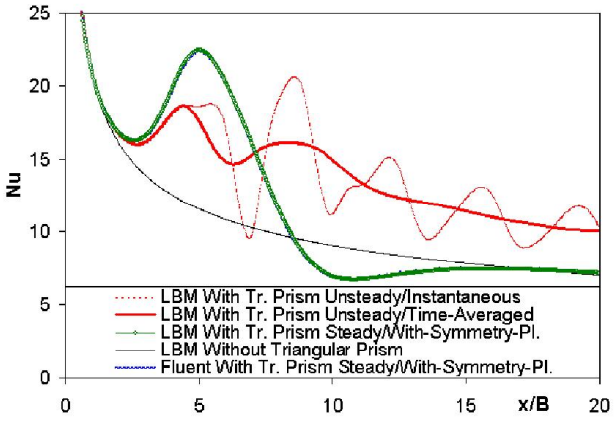

Figure 8 Predicted Nu variations along channel wall, Re = 800.

CONCLUSIONS

LBM is employed to investigate the incompressible, laminar flow and heat transfer for a fluid with constant material properties, in a 2D channel with a triangular prism. The developed LBM code is validated by comparisons with a well-established commercial CFD code. Results show that the presence of a triangular prism affects the flow and heat transfer patterns for the steady-state (lower Re) and unsteady-periodic flow (Re>500) regimes. It is observed that heat transfer can be enhanced by the triangular prism, especially for the high Re flows, exhibiting an unsteady-periodic flow structure. The latter is shown to be the main mechanism responsible for this enhancement. It is also shown that an artificial suppression of flow unsteadiness (e.g. by a symmetry plane) can lead to large errors in the prediction of the time-averaged values.

REFERENCES

[1] Wesfreid, J. E., Goujon-Durand, S., Ziclinska, B. J. A., Global mode behavior of the streamwise velocity in wakes, *Journal of Physics* , Vol. 6, 1996, pp. 1343-1357.

[2] Biswas, G., Laschefski, H., Mitra, N. K. and Fiebig, M., Numerical investigation of mixed convection heat transfer in a horizontal channel with a built-in square cylinder, *Numerical Heat Transfer Part A*, Vol. 18, 1990, pp. 173-188.

[3] Abbasi, H., Turki, S., Ben Nasrallah, S., Numerical investigation of forced Convection in a horizontal channel with a built-in triangular prism, *ASME Journal of Heat Transfer*, Vol. 124, 2002, pp. 571-573.

[4] Chattopadhyay, H., Augmentation of heat transfer in a channel using a triangular prism, *International Journal of Thermal Sciences*, Vol. 46, 2002, pp. 501-505.

[5] Succi, S., *The Lattice Boltzmann Equation for Fluid Dynamics and Beyond*, Clarendon Press, Oxford, 2001.

[6] Benim, A. C., Aslan, E., Taymaz, I., Application of the Lattice Boltzmann Method to Steady Incompressible Laminar High Re Flows, *Proceedings of the 7th IASME/WSEAS International Conference on Fluid Mechanics and Aerodynamics*, Moscow, 2009, pp. 220-225.

[7] Fluent 6.3, *User's Guide*, Fluent Inc., Lebanon, NH, 2009.

[8] Moussaoui, M. A., Mezrhab, A., Naji, H., El Ganaoui, M., Prediction of heat transfer in a plane channel built-in three heated square obstacles using an MRT lattice Boltzmann method, *Proceedings of the "6th International Conference on Computational Heat and Mass Transfer*, Guangzhou, 2009, pp. 176-181.

[9] Bhatnagar, P., Gross, E. and Krook, M., A model for collisional processes in gases I: small amplitude processes in charged and neutral one-component system, *Physical Review*, Vol. 94, 1954, pp. 511-525.

[10] He, X. and Luo, L.-S., Lattice Boltzmann model for the incompressible Navier-Stokes equation, *Journal of Statistical Physics*, Vol. 88, 1997, pp. 927-944.

[11] He, X., Luo, L.-S., Dembo, M., Some progress in the lattice Boltzmann method: Reynolds number enhancement in Simulations, *Journal of Physics A*, Vol. 239, 1997, pp. 276-285.

[12] Wu, H. R., He, Y. L., Tang, G. H., Tao, W. Q., Lattice Boltzmann simulation of flow in porous media on non-uniform grids, *Progress on Computational Fluid Dynamics*, Vol. 5, 2005, pp. 97-103.

[13] D'Humiéres, D, Ginzburg, I., Krafczyk, M., Lallemand, P., Luo, L-S., Multiple-relaxation-time Lattice Boltzmann models in three dimensions, *Philosophical Transactions of the Royal Society London A*, Vol. 360, 2002, pp. 437-451.

[14] Mohammad, A. A., *Applied Lattice Boltzmann Method*, SURE Print, Dalbrent, Canada, 2002.

[15] Bejan, A. *Heat Transfer*, John Wiley & Sons, New York, 1993.